

# Polymer electrolytes composed of lithium tetrakis(pentafluorobenzenethiolato) borate and poly(fluoroalkylcarbon)s

Takahiro Aoki\*, Akinori Konno, Tatsuo Fujinami

*Department of Materials Science and Chemical Engineering, Faculty of Engineering, Shizuoka University, 3-5-1, Johoku, Hamamatsu 432-8561, Japan*

Available online 31 May 2005

## Abstract

Lithium ion conducting polymer electrolytes were prepared by mixing insoluble lithium tetrakis(pentafluorobenzenethiolato) borate (LiTPSB) with poly(vinylidene fluoride) (PVDF) or poly(vinylidene fluoride-co-hexafluoropropylene) (PVDF-HFP). Their films were prepared by hot pressing and are investigated for ionic conductivity and thermal properties. LiTPSB is insoluble in PVDF. Ionic conductivity was largely dependent on the salt content for LiTPSB–PVDF composite polymer electrolytes, and exhibited higher ionic conductivity than homogeneous LiTFSI–PVDF based polymer electrolytes. Melting point and crystallinity of PVDF were independent on LiTPSB content, resulting in no difference for melting point and crystallinity between pure PVDF and LiTPSB–PVDF. Ionic conductivity was effectively improved by incorporation of 18-crown-6 or kryptofix222 for LiTPSB–PVDF based polymer electrolytes.

© 2005 Elsevier B.V. All rights reserved.

**Keywords:** Polymer electrolyte; Poly(vinylidene fluoride); Ionic conductivity; Lithium salt

## 1. Introduction

Dry polymer electrolytes have been attracting interest as safer alternatives to liquid electrolytes and suitable use in lithium secondary batteries [1–3]. Lithium salts which exhibit high dissociation, high electrochemical stability and good thermal stability, are taken important role for high performance polymer electrolytes. Weakly coordinating anions such as lithium bis(oxalato) borate [4], lithium tetrakis(haloacyloxy) borate [5], lithium tris(fluorobenzenediolato) phosphate [6], lithium bis(polyfluorodiolato) borate [7], lithium bis(trifluoroborane) imidazolide [8] and lithium dicyanotriazolate [9] have been investigated.

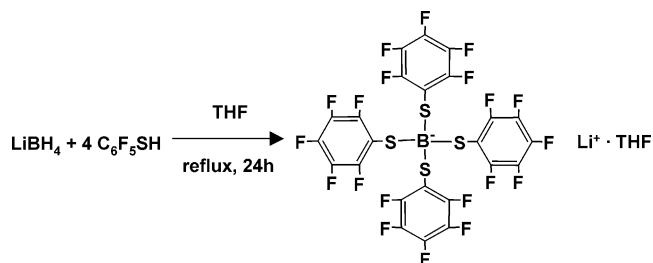
We have reported lithium ion conducting ionic liquid which contain two methoxy [oligo (ethyleneoxide)] and two electron withdrawing groups bonded to aluminate or borate complex center, exhibited high ionic conductivity and

high lithium ion transference numbers [10]. Borates exhibited higher ionic conductivities than corresponding aluminates due to weaker interaction between lithium ion and borate anion [11].

We designed lithium tetrakis(pentafluorobenzenethiolato) borate (LiTPSB) by using the calculations in MOPAC. Poly(fluoroalkylcarbon) such as poly(vinylidene fluoride) (PVDF) and poly(vinylidene fluoride-co-hexafluoropropylene) (PVDF-HFP) show high dielectric constants, good mechanical properties and good electrochemical stabilities to electrode materials such as carbon materials and lithium metal. Weak interaction of lithium ion with fluorine atoms was estimated from small partial negative charge on fluorine atoms in PVDF. Based on these properties, poly(fluoroalkylcarbon)s can be used as host polymers in dry solid electrolytes.

In this paper, we wish to report the ionic conductivity, thermal properties and ion conduction mechanism for heterogeneous LiTPSB–PVDF and LiTPSB–PVDF-HFP polymer electrolytes. In addition, LiTFSI based polymer electrolytes were investigated compared with LiTPSB–PVDF.

\* Corresponding author. Tel.: +81 53 478 1162; fax: +81 53 478 1162.  
E-mail address: [r5345010@ipc.shizuoka.ac.jp](mailto:r5345010@ipc.shizuoka.ac.jp) (T. Aoki).



Scheme 1. Synthesis of LiTPSB.

## 2. Experimental

### 2.1. Materials

Lithium borohydride ( $\text{LiBH}_4$ , 2.0 M solution in THF, Aldrich), pentafluorothiophenol (Lancaster), 18-crown-6 (18C6, Wako) and kryptofix222 ( $\text{N}(\text{CH}_2\text{CH}_2\text{OCH}_2\text{CH}_2\text{OCH}_2\text{CH}_2)_3\text{N}$ , K222, Merck) were used as supplied. LiTFSI (Aldrich) was dried at  $100^\circ\text{C}$  for 24 h under vacuum. PVDF ( $M_w: 5.3 \times 10^5$ ,  $T_m = 171^\circ\text{C}$ , powder, Aldrich) and PVDF-HFP ( $M_w: 4.6 \times 10^5$ ,  $T_m = 160^\circ\text{C}$ , pellet, Aldrich) were dried at  $120^\circ\text{C}$  for 24 h under vacuum. Acetone and THF were dried rigorously before use. Unless otherwise stated, all materials were handled on a dry nitrogen line or in an argon glove box in order to rigorously exclude moisture.

### 2.2. Synthesis of LiTPSB

$\text{LiBH}_4$  (10.0 mmol) and pentafluorothiophenol (40.0 mmol) were refluxed in THF (40 ml) for 24 h (Scheme 1). By volumetric analysis,  $\text{H}_2$  gas (40 mmol) was evolved quantitatively. White solid precipitated in refluxing. Solvent was removed and dried under reduced pressure at  $80^\circ\text{C}$  for 24 h, and white solid was obtained. White powder LiTPSB was obtained by washing repeatedly with dry THF and dried under reduced pressure at  $100^\circ\text{C}$  for 24 h (yield 70%). Complete disappearance of S–H (stretching,  $2600\text{--}2500\text{ cm}^{-1}$ ) and B–H (stretching,  $2410\text{--}2390\text{ cm}^{-1}$ ) groups was confirmed on a FT-IR spectrum [12,13]. Analytical results were as follows.

FT-IR (KBr disc):  $980\text{ cm}^{-1}$  (B–S, stretching). Elemental analysis: found C 38.6%, H 0.8%; calculated for LiTPSB ( $\text{LiBS}_4\text{C}_{24}\text{F}_{20}$ ) C 35.4%, H 0.0%; calculated for LiTPSB-THF ( $\text{LiBS}_4\text{C}_{28}\text{F}_{20}\text{OH}_8$ ) C 38.0%, H 0.9%.

### 2.3. Preparation of polymer electrolyte films

LiTPSB–PVDF and LiTFSI–PVDF based polymer electrolyte films were prepared by hot pressing at  $190^\circ\text{C}$  between PTFE disks using a PTFE spacer to control film thickness (0.4 mm) after mixing PVDF with LiTPSB or LiTFSI in an agate mortar. In the same way, LiTPSB–PVDF–18C6 (LiTPSB:18C6 = 1:1 mol) and LiTPSB–PVDF–K222 (LiTPSB:K222 = 1:1 mol) based polymer electrolyte films were obtained.

It is impossible to mix PVDF-HFP with LiTPSB in a mortar because PVDF-HFP is pellet. Therefore LiTPSB–PVDF-HFP based polymer electrolyte films were prepared by casting method. LiTPSB was dispersed to PVDF-HFP acetone solution by magnetic stirring. The solvent was removed under reduced pressure at  $80^\circ\text{C}$  for 24 h and LiTPSB and PVDF-HFP based polymer electrolytes were obtained. LiTPSB–PVDF-HFP based polymer electrolyte films were prepared by hot pressing at  $180^\circ\text{C}$ . The composition of the polymer electrolyte films is summarized in Table 1.

### 2.4. Measurements

Ionic conductivity was determined by ac impedance measurement in the frequency 1 MHz–0.1 Hz (signal amplitude 10 mV) using a Solartron 1260 frequency response analyzer and 1287 electrochemical interface. Cells consisted of polymer electrolyte films sandwiched between stainless steel electrodes.

The particle size of LiTPSB and the surface of the polymer electrolyte films were observed by scanning electron microscopy (SEM) on a JEOL JSM-5600.

The thermogravimetric analysis (TGA) of lithium salts was carried out in nitrogen flow on a Shimadzu TGA-50 system at a heating rate of  $5^\circ\text{C min}^{-1}$  in the temperature range from room temperature to  $500^\circ\text{C}$ .

Table 1  
Physical appearance of polymer electrolyte films

Sample	LiTPSB (wt.%)	LiTFSI (wt.%)	PVDF (wt.%)	PVDF-HFP (wt.%)	Appearance	Other
LiTPSB–PVDF (10/90)	10		90		Opaque strong film	
LiTPSB–PVDF (30/70)	30		70		Opaque strong film	
LiTPSB–PVDF (50/50)	50		50		Opaque weak film	
LiTPSB–PVDF (70/30)	70		30		Opaque fragile film	
LiTFSI–PVDF (10/90)		10	90		Transparent strong film	
LiTFSI–PVDF (25/75)		25	75		Transparent strong film	
LiTFSI–PVDF (40/60)		40	60		Opaque weak film	
LiTFSI–PVDF (60/40)		60	40		Opaque weak film	
LiTPSB–PVDF-HFP (40/60)	40			60	Opaque weak film	
LiTPSB–PVDF–18C6	50		50		Opaque weak film	Salt:18C6 = 1:1 mol
LiTPSB–PVDF–K222	50		50		Opaque weak film	Salt:K222 = 1:1 mol

Thermal properties of the polymer electrolyte films were determined by differential scanning calorimetry (DSC) on a Perkin-Elmer Pyris 1 differential scanning calorimetry at a scan rate of  $10\text{ }^{\circ}\text{C min}^{-1}$  in the temperature range from  $-80$  to  $200\text{ }^{\circ}\text{C}$ .

Molecular structures were depicted using CAChe version 5.0 (Fujitsu). The structure and partial charge of the chemical samples were refined by performed a pre-optimization calculation in Mechanics using Augmented MM3, followed by performed an optimization calculation in MOPAC using PM5 parameters.

### 3. Results and discussion

#### 3.1. Characterization

LiTPSB was designed to have weaker interaction between lithium ion and TPSB anion. Weaker interaction is estimated by the small partial negative charges on anion obtained from the calculations in MOPAC (Fig. 1). Therefore it is expected that high ionic conductivity will be obtained for LiTPSB based polymer electrolytes.

It is confirmed that LiTPSB is complexed with THF in the ratio of 1 to 1 in this method from elemental analysis. LiTPSB is insoluble in polar and less polar solvents. This can be ascribed to the weaker interaction between TPSB anion and solvents due to delocalization of the negative charge over the anion and it results in insolubility of LiTPSB. Similar insolubility of salt was reported for lithium bis(malonato) borate [4]. Polymer electrolyte films were prepared not by casting method but by hot pressing after mixing lithium salt with host polymers in an agate mortar due to insoluble LiTPSB on this report. White opaque films were obtained for LiTPSB based polymer electrolytes. Transparent films were obtained by incorporation of 10, 25 wt.% lithium salt and white opaque films were obtained by incorporation of 40 and 60 wt.% lithium salt for LiTFSI based polymer electrolytes. Films containing less than 30 wt.% lithium salt were mechanically strong and films containing more than 70 wt.% salt were fragile for LiTPSB or LiTFSI based electrolytes (Table 1).

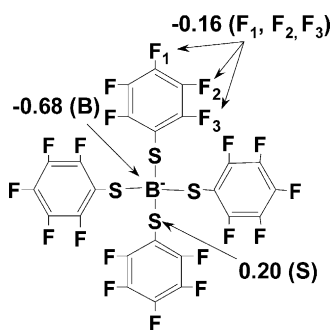


Fig. 1. Partial charge of TPSB anion from the optimization calculations in MOPAC (PM5).

#### 3.2. SEM images

SEM images of grinded LiTPSB particle are shown in Fig. 2. The particle size of LiTPSB distributed from  $100\text{ nm}$  to  $5\text{ }\mu\text{m}$  (Fig. 2a), and the particles looked like an aggregate (Fig. 2b). SEM image of the surface for LiTPSB–PVDF (50/50) film after hot pressing at  $190\text{ }^{\circ}\text{C}$  is shown in Fig. 3. LiTPSB dispersed as particles in polymer electrolyte films.

#### 3.3. Thermal properties

Thermal stability was investigated by TGA measurements in nitrogen flow at a heating rate of a  $5\text{ }^{\circ}\text{C min}^{-1}$  in the temperature range from room temperature to  $500\text{ }^{\circ}\text{C}$ . TGA curves of LiTPSB and LiTFSI are shown in Fig. 4. LiTPSB have two weight loss peaks. First peak of weight loss started from  $200\text{ }^{\circ}\text{C}$ , which can be probably ascribed to the desorption of THF from LiTPSB–THF complex. Second peak of weight loss started from  $350\text{ }^{\circ}\text{C}$ , which can be ascribed to the thermal

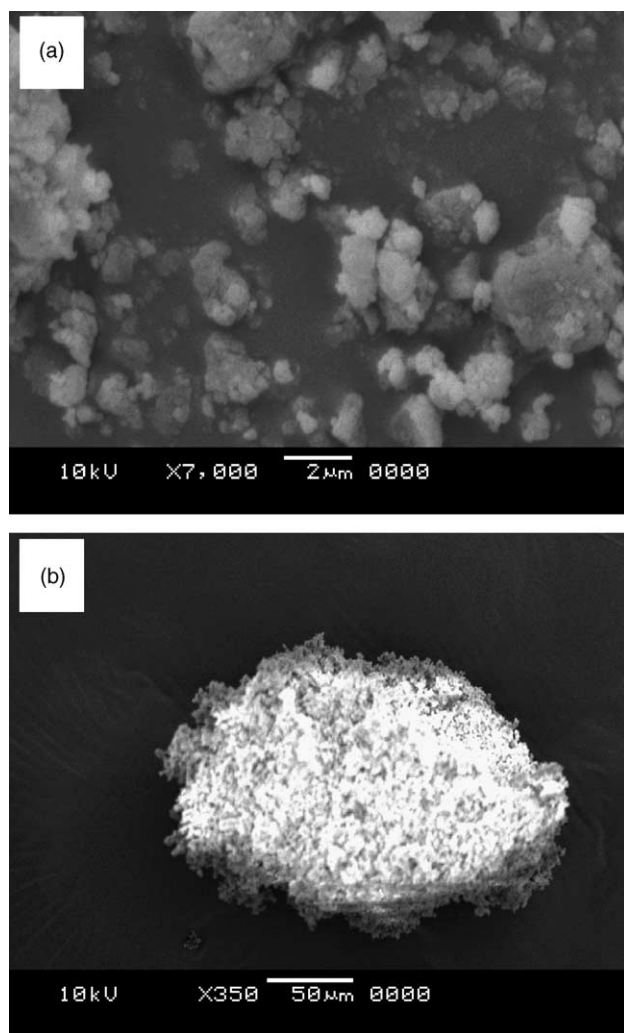


Fig. 2. SEM images of LiTPSB after grinding: (a) minimum particle (<200 nm), (b) aggregate (>100  $\mu\text{m}$ ).

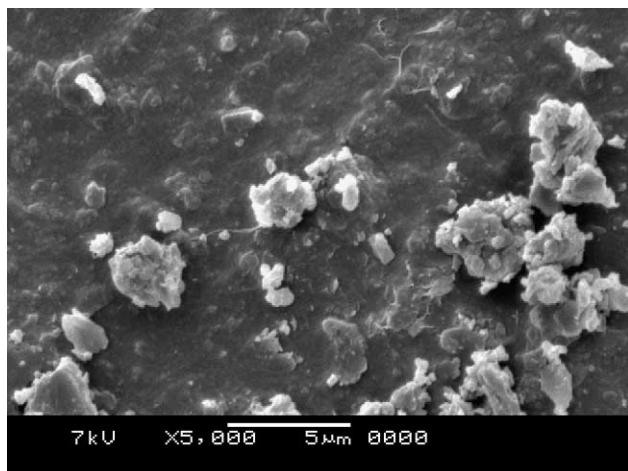


Fig. 3. SEM image of LiTPSB–PVDF (50/50) film.

decomposition of LiTPSB itself. LiTFSI has thermal stability up to 350 °C.

Thermal properties of the polymer electrolyte films were investigated by DSC measurements at a scan rate of 10 °C min<sup>-1</sup> in the temperature range from -80 to 200 °C. Glass transition temperature was not observed for all samples in this temperature range. Melting point and crystallinity ( $\chi$ ) was determined from second heating cycle. The crystallinity of polymer electrolyte films was determined by the following equation:

$$\chi = [\Delta H / \Delta H_{\text{fus}}^{\circ}] / W$$

$\Delta H$  is enthalpy of fusion from DSC measurements,  $\Delta H_{\text{fus}}^{\circ}$  the enthalpy of fusion from complete PVDF crystal and  $W$  the weight ratio of PVDF in samples.  $\Delta H_{\text{fus}}^{\circ}$  was taken as 96.8 J g<sup>-1</sup> [14]. Melting point and crystallinity of LiTPSB based polymer electrolyte films is shown in Table 2. LiTPSB based polymer electrolyte films exhibited melting point of 149.3–150.9 °C and crystallinity of 37–41, and it was recognized that melting point and crystallinity is independent

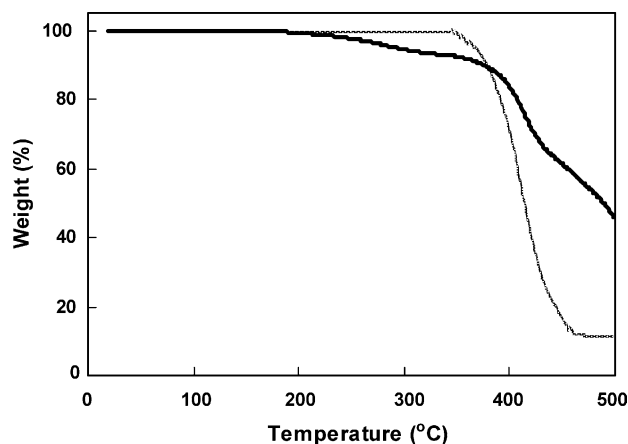


Fig. 4. TGA curves of LiTPSB (—) and LiTFSI (---) at a heating rate of 10 °C min<sup>-1</sup> in N<sub>2</sub> flow.

Table 2  
Melting point ( $T_m$ ) and crystallinity ( $\chi$ ) of polymer electrolyte films based on LiTPSB and PVDF

Salt content (wt.%)	$T_m$ (°C)	Crystallinity (%)
0	150.1	40
10	150.6	38
30	150.9	40
50	150.2	41
70	149.3	37

on the salt content. The crystalline region of PVDF did not change by adding LiTPSB. No change in melting point and crystallinity supported that LiTPSB was absolutely insoluble in PVDF.

### 3.4. Ionic conductivity

LiTPSB is insoluble in any solvents and polymers, and the pressed LiTPSB pellet exhibited very low conductivity of <10<sup>-9</sup> S cm<sup>-1</sup> at 190 °C. However ionic conduction was observed by blending with PVDF. Relationships between salt content and ionic conductivity for LiTPSB–PVDF and LiTFSI–PVDF based polymer electrolytes are shown in Fig. 5a and b, respectively. LiTFSI based polymer electrolyte

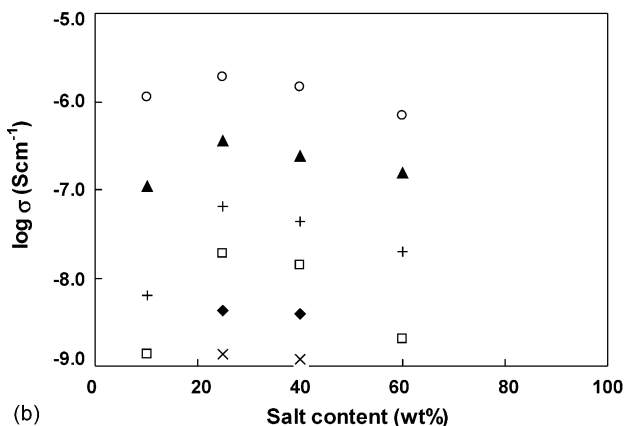
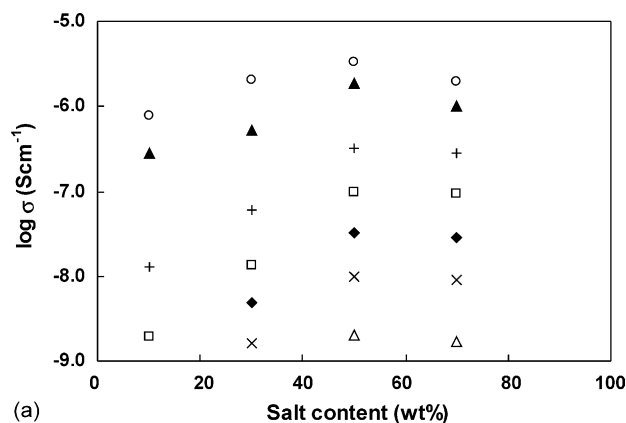


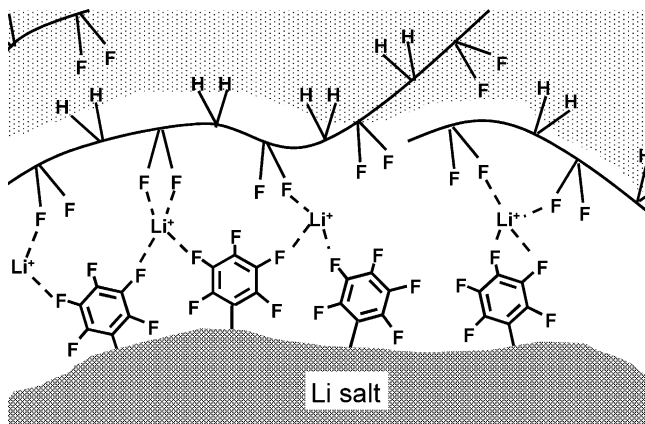
Fig. 5. Relationships between salt content and ionic conductivity for (a) LiTPSB–PVDF systems and (b) LiTFSI–PVDF systems at 190 °C (○), 170 °C (▲), 150 °C (+), 130 °C (□), 110 °C (◆), 90 °C (×) and 70 °C (△).



films containing less than 25 wt.% lithium salt were transparent. On the other hand, LiTPSB–PVDF polymer electrolyte films were white opaque for all salt content. Optimized composition of polymer electrolyte LiTFSI–PVDF (25/75), exhibited ionic conductivities of  $1 \times 10^{-9} \text{ S cm}^{-1}$  at  $90^\circ\text{C}$  and  $2 \times 10^{-6} \text{ S cm}^{-1}$  at  $190^\circ\text{C}$  (Fig. 5b). Optimized composition of polymer electrolyte LiTPSB–PVDF (50/50) exhibited ionic conductivities of  $1 \times 10^{-8} \text{ S cm}^{-1}$  at  $90^\circ\text{C}$  and  $3 \times 10^{-6} \text{ S cm}^{-1}$  at  $190^\circ\text{C}$  (Fig. 5a). Lithium ion is transported in amorphous phase by segment motion for ordinary poly(ether) based polymer electrolytes. On the other hand, it is estimated that lithium ion is not transported in amorphous phase by segment motion for LiTPSB–PVDF system because LiTPSB is insoluble in PVDF. Then, ionic conduction mechanism for this system is proposed in Scheme 2. LiTPSB is insoluble in PVDF and exhibited very low conductivity alone. Therefore, lithium ion transport is possible at the interface between LiTPSB and PVDF. Optimized composition LiTPSB–PVDF (50/50) forms good interfacial conduction pathway between LiTPSB and PVDF. Glass transition temperature at the surface is lower than that at the bulk for polymers [15]. Therefore it is estimated to the increase of lithium ion mobility at the interface due to more flexible polymer chains at the interface, and it resulted in higher ionic conductivity.

Temperature dependence of ionic conductivity for LiTPSB–PVDF (50/50), LiTPSB–PVDF–HFP (40/60) and LiTFSI–PVDF (25/75) is shown in Fig. 6. Ionic conductivity increased as follows, LiTPSB–PVDF–HFP (40/60) > LiTPSB–PVDF (50/50) > LiTFSI–PVDF (25/75). Heterogeneous LiTPSB–PVDF based polymer electrolytes exhibited higher ionic conductivity than LiTFSI–PVDF system.

Temperature dependence of ionic conductivity for LiTPSB–PVDF (50/50), LiTPSB–PVDF–18C6 and LiTPSB–PVDF–K222 is shown in Fig. 7. Ionic conductivity was effectively improved by incorporation of 18C6 or K222. Ionic conductivity increased as following order, LiTPSB–PVDF–18C6  $\cong$  LiTPSB–PVDF–K222 > LiTPSB–



Scheme 2. Interface between insoluble LiTPSB and PVDF.

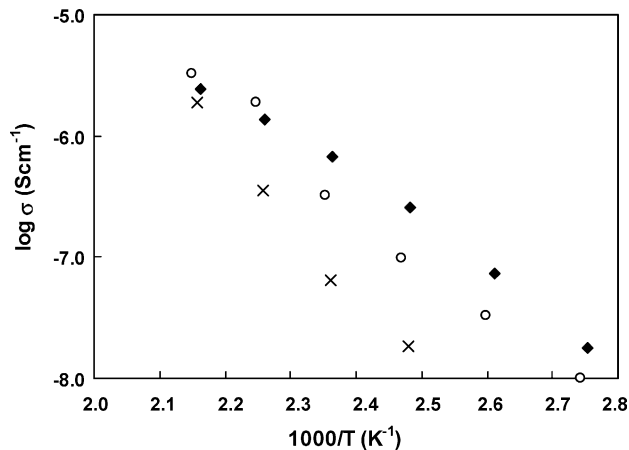


Fig. 6. Temperature dependence of ionic conductivity for LiTPSB–PVDF (50/50) (○), LiTPSB–PVDF–HFP (40/60) (◆) and LiTFSI–PVDF (25/75) (×).

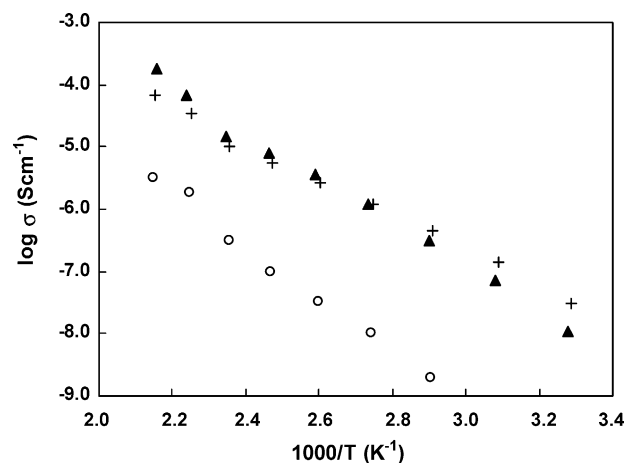


Fig. 7. Temperature dependence of ionic conductivity for LiTPSB–PVDF (50/50) (○), LiTPSB–PVDF–18C6 (+) and LiTPSB–PVDF–K222 (▲).

PVDF (50/50). LiTPSB–PVDF–18C6 exhibited high ionic conductivity of  $1 \times 10^{-6} \text{ S cm}^{-1}$  at  $90^\circ\text{C}$  and  $7 \times 10^{-5} \text{ S cm}^{-1}$  at  $190^\circ\text{C}$ . Large increase in ionic conductivity was observed at about  $170^\circ\text{C}$  for all electrolytes. This phenomenon can be explained to the increase of lithium ion mobility resulted from acceleration of the chain motion in molten polymer.

#### 4. Conclusion

Lithium ion conducting polymer electrolytes were prepared by hot pressing after mixing LiTPSB with PVDF or PVDF–HFP. It was observed that LiTPSB was insoluble but dispersed as the particle in LiTPSB–PVDF films. Ionic conductivity was largely dependent on the salt content in LiTPSB–PVDF polymer electrolytes, which exhibited higher ionic conductivity than LiTFSI–PVDF based polymer electrolytes. Ionic conductivity was effectively improved by incorporation of 18-crown-6 or kryptofix222 for

LiTPSB–PVDF based polymer electrolytes. It is observed that melting point and crystallinity of PVDF did not change as increasing salt content in LiTPSB–PVDF electrolytes because LiTPSB is insoluble in PVDF. Lithium ion transport through the interfacial conduction pathway between LiTPSB and PVDF is tentatively proposed. High ionic conductivity will be obtained by the formation of better interface using smaller particle of LiTPSB.

## References

- [1] F. Croce, G.B. Appetecchi, L. Persi, B. Scrosati, *Nature* 394 (1998) 456.
- [2] M. Watanabe, T. Endo, A. Nishimoto, K. Miura, M. Yanagida, *J. Power Sources* 81–82 (1999) 786.
- [3] Y. Ohseido, I. Imae, Y. Shirota, *Electrochim. Acta* 45 (2000) 1543.
- [4] W. Ku, A.J. Shusterman, R. Marzke, C.A. Angell, *J. Electrochem. Soc.* 151 (2004) A632.
- [5] H. Yamaguchi, H. Takahashi, M. Kato, J. Arai, *J. Electrochem. Soc.* 150 (2003) A312.
- [6] N. Nanbu, K. Tsuchiya, T. Shibasaki, Y. Sasaki, *Electrochem. Solid-State Lett.* 5 (2002) A202.
- [7] B.G. Nolan, S.H. Strauss, *J. Electrochem. Soc.* 150 (2003) A1726.
- [8] T.J. Barbarich, P.F. Driscoll, *Electrochem. Solid-State Lett.* 6 (2003) A113.
- [9] M. Egashira, B. Scrosati, M. Armand, S. Béranger, C. Michot, *Electrochem. Solid-State Lett.* 6 (2003) A71.
- [10] T. Fujinami, Y. Buzoujima, *J. Power Sources* 119 (2003) 438.
- [11] T. Aoki, A. Konno, T. Fujinami, *J. Electrochem. Soc.* 191 (2004) A887.
- [12] S.A.A. Zaidi, M.A. Zahoor, K.S. Siddiqi, *Transition Met. Chem.* 15 (1990) 231.
- [13] K. Onishi, M. Matsumoto, K. Shigehara, *Chem. Mater.* 10 (1998) 927.
- [14] J. Brandrup, E.H. Immergut, E.A. Grulke, *Polymer Handbook*, 4th ed., Wiley-Interscience, p. VI/14.
- [15] K. Tanaka, A. Takahara, T. Kajiyama, *Macromolecules* 33 (2000) 7588.